J. Synchrotron Rad. (2000). **7**, 313–317

Primary radiation damage of protein crystals by an intense synchrotron X-ray beam

Tsu-yi Teng* and Keith Moffat

Department of Biochemistry and Molecular Biology, The University of Chicago, Chicago, IL 60637, USA. E-mail: t-teng@uchicago.edu

(*Received 4 January 2000; accepted 20 June 2000*)

X-ray radiation damage of a lysozyme single crystal by an intense monochromatic beam from a third-generation radiation source at the Advanced Photon Source has been studied. The results show that primary radiation damage is linearly dependent on the X-ray dose even when the crystal is at cryogenic temperatures. The existence of an upper limit for the primary radiation damage was observed. Above the threshold of approximately 1×10^7 Gy, excessive damage of the crystal develops which is interpreted as the onset of secondary and/or tertiary radiation damage. This upper limit of X-ray dose is compared with Henderson's limit [Henderson (1990). *Proc. R. Soc. London*, B**241**, 6–8], and its implication for the amount of useful X-ray diffraction data that can be obtained for crystals of a given scattering power is also discussed.

Keywords: protein crystals; radiation damage; monochromatic radiation.

1. Introduction

Chemical damage of organic materials by X-rays and other forms of ionizing radiation is believed to consist of two tiers of damage: primary and secondary. Primary damage is caused by direct interaction between the radiation beam and electrons. For an X-ray beam, this interaction leads to the ejection of energetic electrons from atoms *via* the photoelectric, Auger and Compton effects. Primary damage may lead to the breaking of chemical bonds by the radiation, thus causing the destruction of molecules. Secondary damage is caused by the reactions of the resulting radiolytic products, *e.g.* free radicals generated by the energetic electrons. When a material in aqueous solution is exposed to ionizing radiation, free radicals can be generated directly, as a result of the solvent atoms absorbing the ionizing radiation, or indirectly, through reaction with products arising from radiolysis of water. In protein crystals, these free radicals diffuse through the crystal, cause further chemical reactions that alter the structure of the molecules in the crystal lattice and damage the intermolecular contacts that stabilize the crystal lattice. Nave (1995) considered the different damage processes taking place in the crystal and evaluated how they induce direct or indirect radiation damage. A third (or tertiary) tier of damage may be evident in crystalline materials. When a sufficient fraction of molecules has been damaged by primary and secondary effects, the crystal lattice may be destabilized and break down even in the absence of further chemical damage. Henderson (1990) describes this as a domino effect.

Primary radiation damage thus depends only on the energy and number of photons absorbed, but secondary damage varies with the nature of the solvent and with factors such as temperature and the presence or absence of free-radical scavengers that affect the mobility and reactivity of the radiolytic products. In crystals, tertiary radiation damage depends on the stability of the crystal lattice.

X-ray radiation damage to protein crystals in macromolecular crystallography was observed from the earliest days of the field (Blake & Phillips, 1962). When synchrotron X-ray sources became widely available, more quantitative studies of X-ray damage to protein crystals were reported (see Watenpaugh, 1991, and references therein; Gonzalez & Nave, 1994; Nave, 1995). Several groups (Moffat *et al.*, 1986; Moffat, 1989; Getzoff *et al.*, 1993; Gonzalez & Nave, 1994) enhanced the extent of chemical radiation damage from less-brilliant second-generation sources such as CHESS, NSLS and Daresbury by employing a focused polychromatic beam and the Laue method. The rate of absorption of photons from such beams is sufficiently high to lead to a significant temperature rise during even a brief exposure (Chen, 1994). This effect may lead to further physical radiation damage that depends on the rate at which energy is deposited in the crystal and not merely on the total energy deposited.

With the development of macromolecular cryocrystallography, it was observed that cooling crystals to liquid-nitrogen temperature 'greatly reduced the radiation damage' (Hope *et al.*, 1988; Teng, 1990; Young & Dewan, 1990). Although both secondary and tertiary damage are greatly reduced at cryotemperatures, primary radiation damage is independent of temperature. Gonzalez & Nave (1994) showed direct evidence for primary radiation damage of protein crystals at cryotemperatures by polychromatic radiation. However, the common belief was that

excellent monochromatic data sets could be acquired at cryotemperatures before significant chemical or physical radiation damage occurred (Young & Dewan, 1990; Watenpaugh, 1991). This belief has been cast into doubt with the advent of more-brilliant focused monochromatic insertion-device beams from third-generation sources. The wide adoption of cryocrystallographic techniques (Garman & Schneider, 1997) and the much shorter exposures in principle available from such sources mean that primary radiation damage becomes the dominant damage phenomenon. This is particularly evident when ever-smaller microcrystals are examined.

Based on experience (Chiu *et al.*, 1986) that electron diffraction patterns of a wide variety of biological samples lose half of their intensity after 5 electrons $Å^{-2}$ irradiation at 77 K, Henderson (1990) predicted a limit on the absorbed energy of 2×10^7 Gy before significant radiation damage occurs, on illumination by hard X-rays. Since secondary and tertiary radiation damage can be minimized (if not completely eliminated) by certain experimental techniques but primary damage is fixed and inescapable, we examine its effect here for monochromatic radiation and seek to establish the existence of the limit proposed by Henderson (1990). This limit in turn imposes an upper limit on the number of images that can be acquired from a crystal of given scattering power.

2. Materials and methods

Tetragonal crystals of hen egg-white lysozyme (Sigma Chemical Corporation, St. Louis, USA) were grown as described (Drenth, 1994). A crystal of about $100 \times 100 \times 40$ μm was transferred to a cryoprotectant consisting of 5 g PEG (molecular weight 20 000) in 20 ml acetate buffer and flash cooled by immersion in liquid propane at 100 K. The crystal was maintained at 100 ± 1 K during the experiment.

The X-ray experiments were conducted at the BioCARS beamline 14-BM-C at the Advanced Photon Source (APS), Argonne National Laboratory, USA. This beamline accepts approximately 1.2 mrad of radiation from the APS bending-magnet radiation fan and delivers a monochromatic flux of 2.2×10^{11} photons s^{-1} to the crystal with a beam profile of 230 μm (2σ, vertical) $\times$ 250 μm (2σ, horizontal) in a bandpass of 5×10^{-4}. For the experiment, the monochromator was tuned to 12.4 keV (1.0 Å). The crystal was mounted on a Huber Kappa-geometry diffractometer (Huber Diffraktionstechnik GmbH, Rimsting, Germany) and the diffraction data were recorded on an ADSC Quantum-4 CCD detector (Advanced Detector System Corporation, San Diego, USA). The APS storage ring was refilled twice a day. During a fill, the current decays from 100 mA to less than 70 mA. The X-ray photon flux (photons s^{-1}) was measured by a calibrated ion chamber at the crystal position both before and after the refill. The beam profile was measured by scanning a slit–photodiode assembly at the position of the crystal. The peak X-ray intensity was 2.4×10^{12} photons s^{-1} mm^{-2} at 100 mA. The number of photons absorbed per second by the crystal was then calculated from the incident intensity, the mass absorption coefficient of the crystal and its cross-sectional area. The energy deposited was finally calculated from the total exposure time, the energy of each photon and the mass of the crystal. The adiabatic heating rate due to X-ray absorption was calculated to be 0.2 K s^{-1} and physical radiation damage is therefore insignificant in these experiments.

A 10 s exposure of the crystal with a 1.0° oscillation yielded an excellent diffraction image to 1.5 Å resolution. A data set consisting of 100 images required 1000 s of X-ray exposure. Prior to the acquisition of the next data set, the crystal was continuously exposed to X-rays for another 800 s and rotated to ensure even irradiation. Eight data sets were acquired within 8 h during which the accumulated X-ray exposure of the crystal was 1.36×10^4 s. Data were processed using *DENZO* and *SCALEPACK* (Otwinowski & Minor, 1997). All input parameters were identical for each data set. The highest resolution was limited to 1.6 Å (Table 1).

3. Results and discussion

Fig. 1 shows the first and last diffraction images of a lysozyme crystal during a total of 1.36×10^4 s X-ray exposure at 100 K. The inserts show its corresponding visible images, in which an originally perfect crystal becomes opaque and loses its sharp edges.

The deterioration due to radiation damage to the crystal is also immediately evident in several parameters characteristic of the diffraction data. The *R*-factor in the shell of highest resolution increased from 11.8% to 23.1% (Table 1); the unit-cell volume increased by about 0.5% from 2.128×10^5 $Å^3$ to 2.138×10^5 $Å^3$ (Fig. 2*a*), and the overall *B*-factor derived from Wilson plots increased from 13.5 to 17.9 $Å^2$ (Fig. 2*b*). A more detailed inspection of the diffraction data bears out this overall picture. Fig. 3 displays the $\langle I \rangle / \langle \sigma(I) \rangle$ distribution in the highest-resolution shell (1.66 to 1.60 A) for the first, one intermediate and last data sets. After 1.6×10^7 Gy of radiation, the peak of the $\langle I \rangle / \langle \sigma(I) \rangle$ distribution shifted markedly from 35 to 10. In a given resolution range, two further quantities were derived: the summed integrated intensity of all reflections, and the fraction of reflections whose intensities exceeded 20σ. Both quantities are displayed as a function of absorbed dose, in Figs. 2(*c*) and 2(*d*).

A striking quantitative feature of the radiation effects on several parameters characteristic of the diffraction data quality is their closely linear dependence on the absorbed dose, up to a threshold value of approximately 1×10^7 Gy (Figs. 2*b*, 2*c* and 2*d*). At higher absorbed dose, damage exceeds that predicted from the simple linear model: secondary and perhaps tertiary radiation damage effects are becoming significant.

The threshold of approximately 1×10^7 Gy we observe may be compared with Henderson's predicted value of $2 \times$

Table 1
Diffraction data processing.

Overall: reflection from 100 to 1.6 Å. Last shell: reflection from 1.66 to 1.6 Å. $R_{merge} = \Sigma[ABS(I - \langle I \rangle)]/\Sigma(I)$.

Data set	1	2	3	4	5	6	7	8
Total measurement	177002	176679	176880	177623	177971	177501	177530	177465
Unique reflections	14808	14849	14893	14892	14904	14874	14901	14882
Completeness								
Last shell	1.000	0.995	0.979	0.991	0.988	1.000	0.997	0.999
Overall	0.995	0.996	0.994	0.996	0.996	0.998	0.998	0.999
R_{merge}								
Last shell	0.118	0.124	0.132	0.142	0.154	0.173	0.209	0.231
Overall	0.048	0.044	0.044	0.045	0.047	0.048	0.068	0.057
$\langle I \rangle / \langle \sigma(I) \rangle$								
Last shell	24.4	22.2	20.6	19.0	17.6	16.0	13.3	11.8
Overall	37.3	36.7	36.4	36.1	36.0	35.6	34.8	34.2

10^7 Gy (Henderson, 1990), a factor of two larger. Two main sources account for this difference. First, Henderson assumed that the extent of primary damage depends solely on the amount of energy deposited and is independent of whether this energy is derived from the absorption of energetic electrons or hard X-rays. This assumption may not be correct. Second, he assumed very substantial loss of structure whereas we have imposed a much more stringent limit that requires retention of 50% of excellent data in the highest-resolution shell (Figs. 2*c* and 2*d*). From a practical point of view, a crystal is declared 'dead' when it can no longer yield diffraction data of a quality and quantity sufficient to solve a structure or a structural problem. For crystals of the scattering power of lysozyme, if the completeness of the 2 Å shell falls to below 80% the crystal might be declared 'dead'. After 1.36×10^4 s of X-ray exposure, the overall completeness and quality of the data sets from the lysozyme crystal were still high (see Table 1). The crystal was clearly damaged (Fig. 1), its diffraction quality was distinctly degraded (Fig. 2, Table 1), but it was not 'dead'. How many lysozyme molecules were damaged when the threshold was reached in our experiment? The threshold corresponds to the absorption of 3.3×10^{12} photons in a crystal containing 1.9×10^{12} unit cells and 1.5×10^{13} molecules; that is, to roughly 1.7 photons per unit cell and 0.2 photons per molecule.

Henderson's limit, supported experimentally by Gonzalez & Nave (1994) for polychromatic radiation and here for monochromatic radiation, is based on very general considerations and is likely to be widely applicable, since its magnitude depends ultimately on the ratio of the total energy elastically scattered (generating the Bragg peaks) to

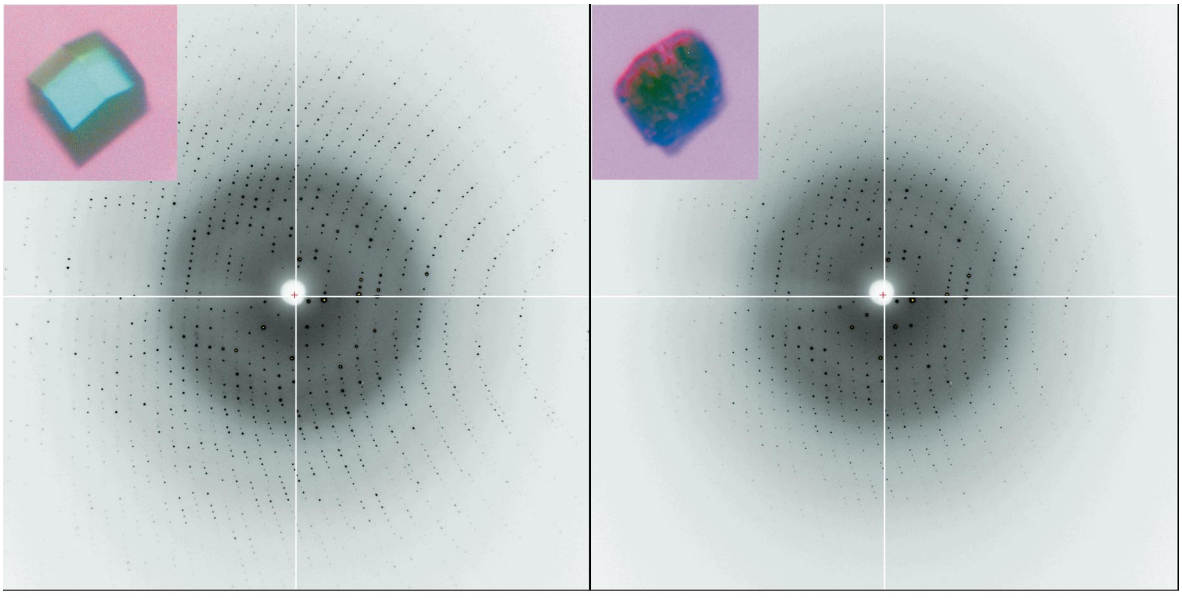

Figure 1
Diffraction images of a lysozyme crystal during a 1.36×10^3 s X-ray exposure at the 14-BM-C beamline. The resolution of diffraction is 1.6 Å at the edge of the image. Two images were taken with identical X-ray dosage. (*a*) The first image; during its exposure 1.2×10^4 Gy were absorbed. (*b*) The last image; after accumulating 1.6×10^7 Gy of absorbed energy. The inserts are photomicrographs of the crystal before and after X-ray exposures. The size of this crystal is $\sim 110 \times 110 \times 60$ µm. The crystal was maintained at 100 ± 1 K during the experiment.

the total energy absorbed (generating primary radiation damage). To generalize the Henderson limit to other crystals, consider the crystal scattering power Σ. Here, Σ, a dimensionless quantity, is given by (Moffat *et al.*, 1986; also see Drenth, 1994)

$$\Sigma = \lambda^3 V_{\rm cryst}(\Sigma f_i^2/V^2),$$

where λ is the X-ray wavelength, $V_{\rm cryst}$ is the volume of the crystal, V is the unit-cell volume, f_i is the atomic scattering factor of the ith atom and the summation is taken over all atoms in the unit cell. For proteins,

$$\Sigma f_i^2/V^2 \simeq 3.2/V_m V,$$

where V_m is the Matthews parameter and hence

$$\begin{aligned}\Sigma &\simeq 3.2\lambda^3(V_{\rm cryst}/V)/V_m \\ &= 3.2\lambda^3 N/V_m,\end{aligned}$$

where N is the number of unit cells in the crystal. The total energy E reflected into a typical Bragg reflection is proportional to Σ and to the incident X-ray intensity (Moffat *et al.*, 1986; also see Drenth, 1994).

The lysozyme crystal used in our experiment had a Σ value of 3.3×10^{12} and yielded five complete data sets before the primary radiation damage limit was reached, and (we estimate) could have yielded ten usable data sets before being declared 'dead'. If the total energy E reflected into a typical Bragg reflection is to be maintained, a crystal of one-tenth the volume (*e.g.* $35 \times 35 \times 35$ µm) would require ten times the exposure per image and would yield one complete data set; and a crystal of one-hundredth the volume (*e.g.* $8 \times 8 \times 8$ µm) would yield only one image. We conclude that (other factors being equal) the value of Σ for a crystal of this absorption coefficient must exceed 3×10^{11} for one data set of 100 images to be obtained, and must exceed 3×10^{10} for one image to be obtained. That is, the existence of a primary radiation damage threshold imposes a lower limit on the crystal scattering power (in this example, determined by the crystal volume) from which a single good data set or a single good image can be recorded. Gonzalez & Nave (1994) reached the same conclusion from their studies with polychromatic radiation.

We note that a focused undulator beamline at the APS can deliver an intensity sufficiently high that thermal physical damage rather than the primary chemical radiation damage studied here limits the crystal lifetime. If the heating rate due to X-ray absorption exceeds the maximum cooling rate of a few hundred degrees per second (Teng & Moffat, 1998), the crystal temperature will rise without limit and rapidly destroy the crystal by physical radiation

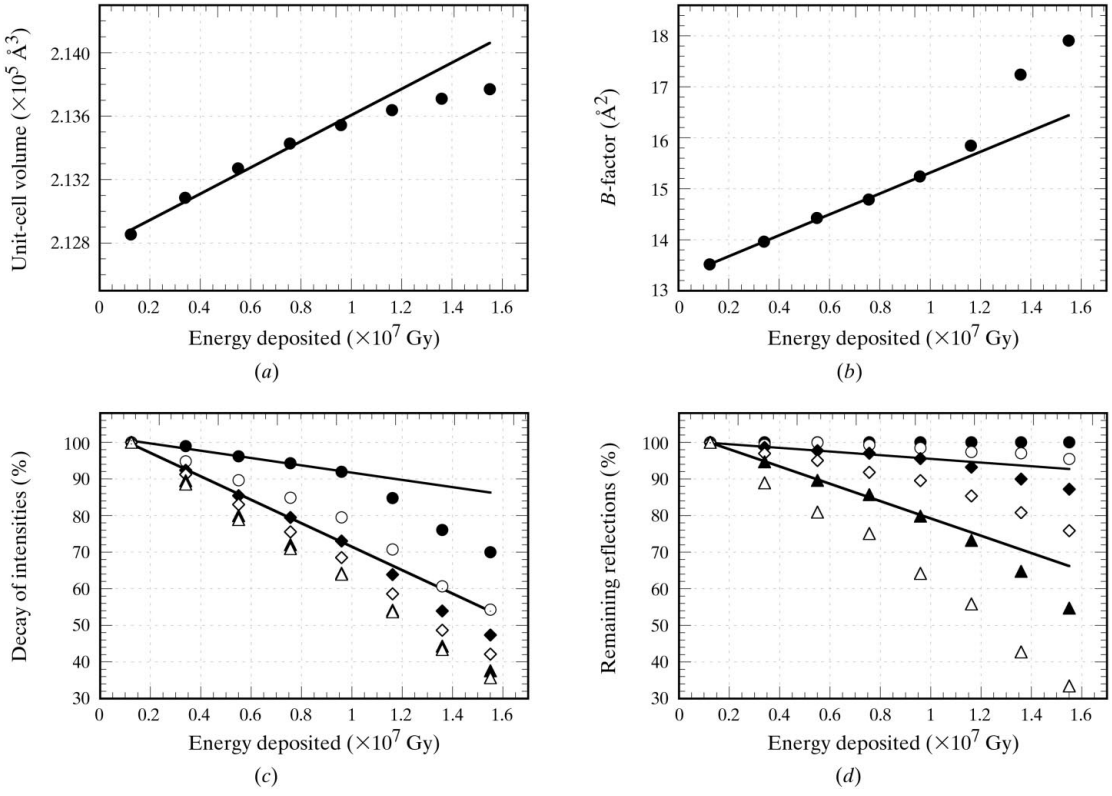

Figure 2
Physical values and parameters of the data sets plotted as a function of absorbed energies during the experiment. (*a*) Unit-cell volume of the crystal. (*b*) *B*-factor extrapolated from Wilson plots of the data. (*c*) Total diffraction intensity. The intensities were summed up according to resolution bins. (*d*) Number of reflections with $I/\sigma(I) > 20$ in each resolution bin. The data in panels (*c*) and (*d*) are plotted as a percentage compared with the first data set in the experiment. For clarity, only six of the ten resolution bins are presented in the plots. ●, 100 to 3.45 Å; ○, 3.45 to 2.74 Å; ◆, 2.39 to 2.17 Å; ◇, 2.02 to 1.90 Å; ▲, 1.80 to 1.72 Å; △, 1.66 to 1.60 Å. The crystal was maintained at 100 ± 1 K during the experiment.

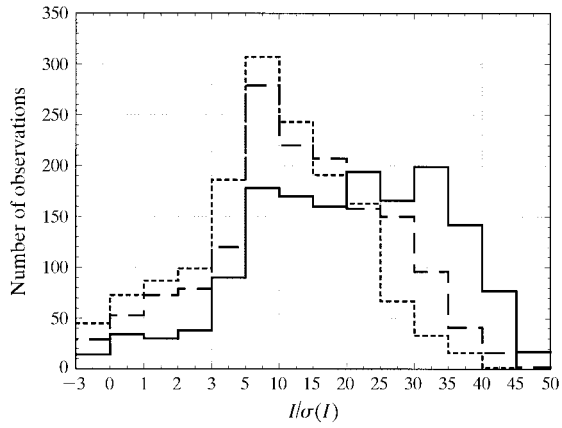

Figure 3
The $I/\sigma(I)$ distribution for the highest-resolution bin (1.66–1.60 A) for three data sets. Solid line: the first set, accumulated energy absorbed 1.2×10^6 Gy; dotted line: the last set, accumulated energy absorbed 1.6×10^7 Gy; dashed line: the sixth set, accumulated energy absorbed 1.1×10^7 Gy.

damage (Garman, 1999). Walsh *et al.* (1999) both defocused and attenuated the monochromatic beam emitted by an APS undulator A by a factor of ~100 (see also Garman, 1999) which minimized thermal effects. Studies of radiation damage of proteins at both lower and higher temperatures are underway.

Finally, primary radiation damage effects, which are by definition local, will be concentrated around atoms with higher mass absorption coefficients such as sulfur (Weik *et al.*, 2000), metal centers and the heavy atoms in heavy-atom derivatives. They are, of course, also evident in solution experiments such as EXAFS spectroscopy (see *e.g.* Murphy *et al.*, 1995) and may produce redox changes at metal centers (see *e.g.* Debenham *et al.*, 1996).

Note added in proof: After the completion of our manuscript, two comprehensive studies (Ravelli & McSweeney, 2000; Burmeister, 2000) on X-ray damage of proteins have been published. Although these studies, like ours, describe the effects of radiation damage globally, in reciprocal space, they concentrate on specific damages, in real space. Our results largely agree with theirs. For example, if a linear fit is used instead of an exponential fit, in the lower dose region a limit of 1.3×10^7 Gy was drawn from Burmeister (2000; Fig. 2) in agreement with our value of 1×10^7 Gy. Also, our calculated crystal size ($35 \times 35 \times 35$ μm) needed for a good data set agrees with the size of $30 \times 30 \times 30$ μm estimated from 'day-to-day experience' by Burmeister (2000).

TYT thanks Vukica Srajer and Marius Schmidt for many discussions and Reinhard Pahl for help in photon flux measurement. We thank all BioCARS staff for their excellent support. Use of the Advanced Photon Source was supported by the US Department of Energy, Basic Energy Sciences, Office of Science, under Contract No. W-31-109-Eng-38. Use of the BioCARS Sector 14 was supported by the National Institutes of Health, National Center for Research Resources, under grant number RR07707.

References

Blake, C. C. F. & Phillips, D. C. (1962). In *Biological Effects of Ionizing Radiation at the Molecular Level*, pp. 183–191. Symposium held by the International Atomic Energy Agency, Brno, Czechoslovakia, 2–6 July 1962. Vienna: IAEA.
Burmeister, W. P. (2000). *Acta Cryst.* D**56**, 328–341.
Chen, Y. (1994). PhD thesis, Cornell University, USA.
Chiu, W., Downing, K. H., Dubochet, J., Glaeser, R. M., Heide, H. G., Knapek, E., Kopf, D. A., Lamvik, M. K., Lepault, J., Robertson, D., Zeitler, E. & Zemlin, F. (1986). *J. Microsc.* **144**, 385–391.
Debenham, M. J., Hao, Q., Hasnain, S. S., Dodd, F. E., Abraham, Z. H. L. & Eady, R. R. (1996). *J. Synchrotron Rad.* **3**, 14–19.
Drenth, J. (1994). *Principles of Protein X-ray Crystallography*. Berlin: Springer.
Garman, E. F. (1999). *Acta Cryst.* D**55**, 1641–1653.
Garman, E. F. & Schneider, T. R. (1997). *J. Appl. Cryst.* **30**, 211–237.
Getzoff, E. D., Jones, K. W., McRee, D., Moffat, K., Ng, K., Rivers, M. L., Schildkamp, W., Singer, P. T., Spanne, P., Sweet, R. M., Teng, T.-Y. & Westbrook, E. M. (1993). *Nucl. Instrum. Methods*, B**79**, 249–255.
Gonzalez, A. & Nave, C. (1994). *Acta Cryst.* D**50**, 874–877.
Henderson, R. (1990). *Proc. R. Soc. London*, B**241**, 6–8.
Hope, H. (1988). *Acta Cryst.* B**44**, 22–26.
Moffat, K. (1989). *Annu. Rev. Biophys. Biophys. Chem.* **18**, 309–332.
Moffat, K., Bilderback, D., Schildkamp, W. & Volz, K. (1986). *Nucl. Instrum Methods*, A**26**, 627–635.
Murphy, L. M., Dobson, B. R., Neu, M., Ramsdale, C. A., Strange, R. W. & Hasnain, S. S. (1995). *J. Synchrotron Rad.* **2**, 64–69.
Nave, C. (1995). *Radiat. Phys. Chem.* **45**, 483–490.
Otwinowski, Z. & Minor, W. (1997). *Methods Enzymol.* **276**, 307–326.
Ravelli, R. B. G. & McSweeney, S. M. (2000). *Structure*, **8**, 315–328.
Teng, T.-Y. (1990). *J. Appl. Cryst.* **23**, 387–391.
Teng, T.-Y. & Moffat, K. (1998). *J. Appl. Cryst.* **31**, 252–257.
Walsh, M. A., Dementieva, I., Evans, G., Sanishvili, R. & Joachimiak, A. (1999). *Acta Cryst.* D**55**, 1168–1173.
Watenpaugh, K. (1991). *Curr. Opin Struct. Biol.* **1**, 1012–1015.
Weik, M., Ravelli, R. B. G., Kryger, G., McSweeney, S., Raves, M. L., Harel, M., Gros, P., Silman, I., Kroon, J. & Sussman, J. (2000). *Proc. Nat. Acad. Sci. USA*, **97**, 623–628.
Young, A. C. M. & Dewan, J. C. (1990). *J. Appl. Cryst.* **23**, 215–218.